Astron. Astrophys. 351, 573–581 (1999)

ASTRONOMY AND ASTROPHYSICS

Spectroscopy and photometry of the pre-cataclysmic binary PG1026+002⋆

Albert Bruch[1] **and Marcos P. Diaz**[2]

[1] Laboratório Nacional de Astrofísica, CP 21, 37500-000 Itajubá – MG, Brazil
[2] Instituto Astronômico e Geofísico, Universidade de São Paulo, CP 3386, 01060-970 São Paulo – SP, Brazil

Received 6 May 1999 / Accepted 13 September 1999

Abstract. Time resolved spectroscopic and photometric observations of the pre-cataclysmic binary PG1026+002 are presented. An improved orbital period is derived from radial velocity measurements of the Hα emission component. The phasing of the variations of the equivalent width of this line confirms the suspicion expressed by Saffer et al. (1993) that the emission is intrinsic to the red dwarf and not due to a reflection effect as observed in several other pre-cataclysmic binaries. The very slight variations in the light curve detected in our photometric observations can, however, excellently be modeled as being caused by illumination of the secondary by the primary white dwarf.

Key words: stars: variables: general – stars: individual: PG1026+002

1. Introduction

The study of stellar evolution has been one of the great issues of astrophysics in the second half of the twentieth century. While a lot of progress has been achieved in understanding how single stars evolve, many questions remain open concerning the evolution of binary stars, in particular in those cases where the initial component separation is small enough to permit a noticeable perturbation of the evolution of one component by the other at least during certain phases of the lifetime of the system.

A particularly spectacular outcome of binary evolution are cataclysmic variables which are believed to be the results of a common envelope (CE) evolution of an initially much wider binary system: during its red giant or asymptotic branch phase the more massive primary component expands to a degree where it engulfs the less massive secondary which is still on the main sequence. Frictional energy and angular momentum loss helps to expel the common envelope and at the same time causes a substantial shrinking of the binary orbit. One of the possible results of this evolutionary phase is a detached white dwarf – red dwarf pair in a close orbit which may further shrink on longer time scales due to angular momentum loss via gravitational radiation and magnetic breaking until the Roche lobe of the secondary gets into contact with the surface of the red dwarf and stable mass transfer from the secondary to the primary is initiated, giving rise to cataclysmic activity.

Systems in an evolutionary stage between the common envelope phase and the first appearance as cataclysmic variables are called pre-cataclysmic binaries (PCBs) if their evolutionary time scales in this configuration is less or of the order of the Hubble time. Obviously, the determination of the physical and geometrical properties of PCBs as well as their distribution can teach us equally much about the so far not well understood CE phase and about the initial states of cataclysmic variables. One of the principal obstacles in this context is the small number of known PCBs and consequently of reliably determined system parameters, hampering any statistical investigation. The study of individual PCBs is therefore of considerable interest in order to increase the statistical ensemble and finally to get insight into some important stages of binary star evolution.

It may be a matter of taste if the system PG1026+002 ($V = 13\overset{\mathrm{m}}{.}83$) should be regarded as a post common-envelope binary or a pre-cataclysmic variable. The masses derived by Saffer et al. (1993) together with the orbital period yields a component separation which translates into an evolutionary time scale of $\approx 8 \times 10^{10}$ years before the secondary gets into contact with its Roche-limit if the only angular momentum loss mechanism is gravitational radiation (Landau & Lifshitz 1951). However, as Saffer et al. (1993) pointed out, the suspected magnetic activity of the secondary – confirmed in the present paper – could lead to a substantially shorter evolutionary time scale. Here, we will consider PG1026+002 as a PCB.

It was detected during the Palomar Green Survey (Green et al. 1986) as a DA white dwarf with a composite spectrum. The absolute magnitude is estimated to be $M_V = 12\overset{\mathrm{m}}{.}5$ by Fleming et al. (1986). Sion et al. (1988) derive a radius for the white dwarf of $0.0127\,R_\odot$ which – according to the Hamada-Salpeter relation for carbon composition – corresponds to a mass of $0.58 M_\odot$. They also derive a temperature of 9145 K ($\pm$ 15%) which, however, is in contradiction to the temperature measured by Kepler & Nelan (1993) based on IUE spectra who got $18\,200 \pm 400$ K or $19\,900 \pm 390$ K, depending on whether optical data are also considered or not. An attempt of Fabrika et al. (1997) to detect a magnetic field of PG1026+002 failed. The proper motion is $\mu = 0\overset{\mathrm{s}}{.}091 \pm 0\overset{\mathrm{s}}{.}008\,\mathrm{year}^{-1}$ at a position angle of $\Theta = 140^\circ \pm 5^\circ$ (Thejll et al. 1997).

Send offprint requests to: Albert Bruch (albert@marina.lna.br)

⋆ Based on observations obtained at the LNA/CNPq, Itajubá, Brazil

The only more detailed study of PG1026+002 was published by Saffer et al. (1993). Based on extensive spectroscopy they were able to derive numerous system parameters: A $0.65\,M_\odot$ white dwarf and a $0.22\,M_\odot$ M4 main sequence star revolve around each other in a $14^{\rm h}\,20^{\rm m}$ orbit. The orbital inclination is not well constrained: Saffer et al. (1993) found $\sin i = 0.93 \pm 0.56$. The Hα line consists of a broad absorption and a narrow emission component. Radial velocity variations of the latter can easily be measured and led to the quoted orbital period.

In PCBs the emission component often seen in the core of the hydrogen absorption lines is normally interpreted as due to illumination of the side of the red dwarf facing the hot white dwarf. In this case its equivalent width is expected to have a minimum at the phase of upper conjunction of the secondary. In PG1026+002 this idea fits in with the observations of Saffer et al. (1993). However, they argue that the primary is too cool to cause the observed equivalent width of the Hα emission and its variations. They favour instead an explanation as stellar activity being accidentally in phase with the normally expected reflection effect. Since the activity centres are not necessarily stationary on the stellar surface, as suggested by migrating waves in the light curves of many late type binaries (see Saffer et al. 1993 for references), the equivalent width variations are likely to have a different phasing with respect to the binary orbit at other epochs if this scenario is correct.

In order to resolve this question we performed additional spectroscopy of PG1026+002. Another indication of the presence or absence of a noticeable reflection effect in the system would obviously be a corresponding variation in the light curve. Time resolved photometry of PG1026+002 not having yet been published, we therefore also made an effort to observe the orbital light curve. We present our results in this communication.

After the present study was completed we got knowledge of a paper by Wood et al. (1999) which discusses seven spectra of PG1026+002 in the range of Hβ. They updated the orbital period and got a value very close to the one derived in Sect. 3.2, although not quite as accurate. Moreover, the equivalent width variations of the Hβ emission component in their spectra are not in phase with the expectations if they were due to illumination. Therefore Wood et al. (1999) agree with Saffer et al. (1993) that the emission lines are probably due to stellar activity.

2. Observations

All observations were performed at the Laboratório Nacional de Astrofísica (LNA) on Pico dos Dias, Brazil. A finding chart of PG1026+002 based on the STScI Digitized Sky Survey, where also the comparison stars used for our photometric observations are marked, is shown in Fig. 1.

Intermediate resolution spectra (2.5 Å FWHM) in the range of 5 800 Å– 7 120 Å were obtained during three consecutive nights in 1998, February, at the 1.6 m telescope of the LNA. A Cassegrain spectrograph and a narrow slit were employed, sampling the instrumental point-spread function by 2.1 pixels on the CCD detector. They were reduced using normal procedures.

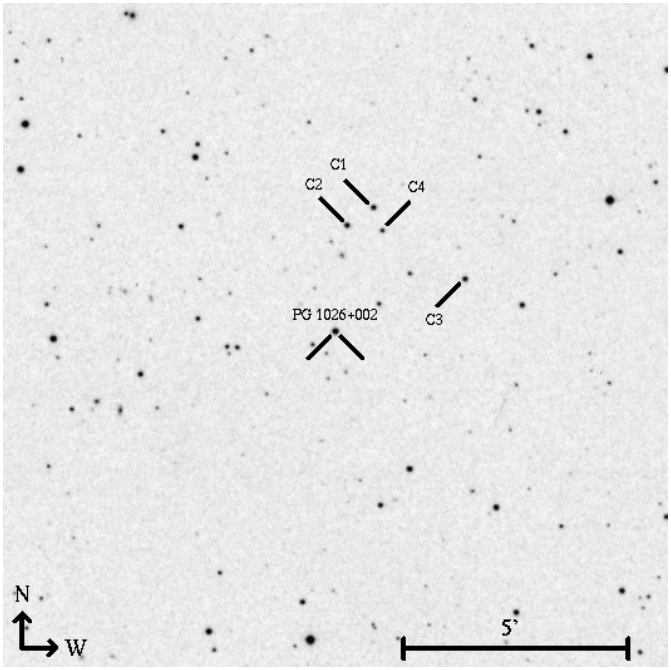

Fig. 1. Finding chart for PG1026+002.

Since the observing conditions were not photometric an absolute flux calibration was not possible. However, observations of some standard stars from the list of Hamuy et al. (1992), enabled the determination of the instrumental sensitivity function and a correction for atmospheric extinction (using the mean extinction curve for the LNA), and thus the reduction of the spectra to a relative flux scale.

The photometric observations were obtained in eight nights also in 1998, February (one night simultaneously with the spectroscopy) through an R filter (Cape system), using the 0.6 m telescope of the Instituto Astronômico e Geofísico, University of São Paulo, located at the LNA. Integration times varied from night to night between $30^{\rm s}$ and $60^{\rm s}$. The dead time between the integrations was about $8^{\rm s}$. A back-illuminated EEV CCD served as detector. After bias subtraction and flat-fielding light curves were constructed non-interactively using the IRAF script LCURVE, which makes use of DAOPHOT/APPHOT routines. Four stars in the vicinity of PG1026+002 – identified in Fig. 1 – were used as comparison stars. Their respective magnitude differences revealed no variability. Since the observing conditions were generally non-photometric, no attempt of an absolute calibration was made. The final light curves are given as magnitude differences Δm between PG1026+002 and the brightest comparison star (C_1). The rms-scatter of the individual Δm values (after subtraction of the orbital variations to be discussed in Sect. 4.1) is $0\overset{\rm m}{.}011$.

Whereas the basic reductions have all been performed using IRAF, the subsequent analysis was done using routines of the MIRA software package (Bruch 1993). A complete journal of the observations is given in Table 1. The orbital phases in the table are based on the ephemeris derived in Sect. 3.2.

Table 1. Journal of observations of PG1026+002

Date	HJD (2 450 000+)	Orbital phase	Number of integrations	Integration Time (s)
Spectroscopy:				
1998 Feb 19	863.647 – 0.779	0.797–1.018	13	900
1998 Feb 20	864.660 – 0.805	0.493–0.736	14	900
1998 Feb 21	865.711 – 0.769	0.253–0.350	4	900
Photometry:				
1998 Feb 1	845.595 – 0.775	0.571–0.872	265	45
1998 Feb 2	846.571 – 0.828	0.205–0.635	379	45
1998 Feb 3	847.720 – 0.826	0.129–0.306	127	60
1998 Feb 4	848.714 – 0.842	0.793–1.007	199	45
1998 Feb 5	849.713 – 0.843	0.466–0.983	136	45
1998 Feb 7	851.664 – 0.827	0.732–1.005	309	30
1998 Feb 19	863.631 – 0.794	0.769–1.042	198	60

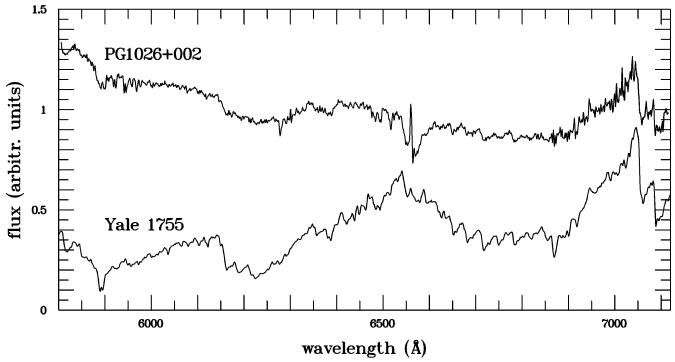

Fig. 2. Mean spectrum of PG1026+002 and the M5 V standard star Yale 1955. The latter has been scaled by an arbitrary factor to fit into the figure.

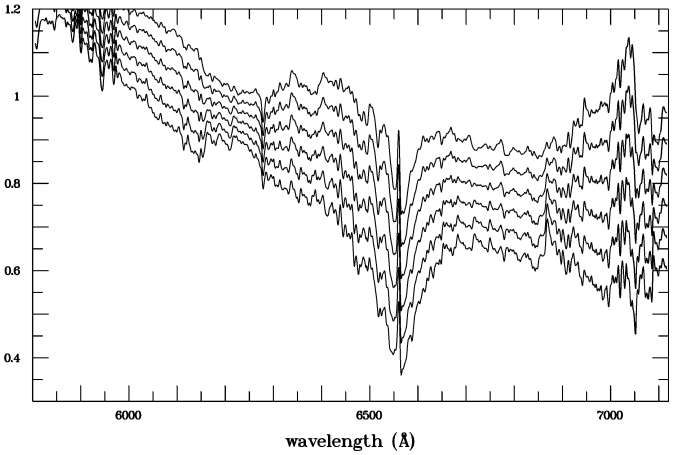

Fig. 3. Spectrum of PG1026+001 after subtraction of different fractions of the M5 V standard star Yale 1755: From top to bottom the subtracted light corresponds to 0.1, 0.15, 0.2, 0.25, 0.3 and 0.35 of the total light at λ = 6700 Å.

3. Spectral analysis

The mean spectrum of PG1026+002 is shown in Fig. 2 along with a scaled spectrum of the M5 V standard star Yale 1755. The latter was taken from Jacoby et al. (1984). The shape of the continuum clearly indicates that blue-ward of Hα the white dwarf dominates, while further to the red the secondary star is brighter. Apart from the broad absorption line of Hα and the embedded narrow emission component the line features as well as the broad spectral bands are due to the late type secondary. Using spectrophotometric measurements up to the near infrared, Saffer et al. (1993) could determine the spectral type of the secondary in PG1026+002 quite accurately. Since the present spectra are restricted to a much narrower wavelength range, it will hardly be possible to improve their classification of M4 which we will adopt in the following.

3.1. Spectral decomposition

In order to determine the fractional contribution of the secondary star to the total light of PG1026+002, and in order to be able to remove the secondary star structures from the profile of the Hα absorption line, the spectrum of Yale 1755 of Jacoby et al. (1984), available in digital form, was multiplied by a suitable factor f and subtracted from PG1026+002. The resolution of the PG1026+002 spectrum was degraded by a Gaussian filter in order to match the lower resolution of the comparison star before this operation. We are aware that the spectrum of Yale 1755 is not ideally suited for this purpose since it is of type M5 V while the secondary of PG1026+002 is classified as a M4 dwarf (Saffer et al. 1993). However, no more suitable comparison spectrum being available, Yale 1755 is the best approximation.

In Fig. 3 the results of the secondary star subtraction for various values of f are shown. None of them is completely satisfactory. In particular, the strong TiO bands around 7 000 Å can only (approximately) be removed at the cost of grossly overcompensating the TiO 6159 Å (band-head) band. The best compromise appears to be the third graph from top in Fig. 3 which was calculated assuming the secondary to contribute 20% of the

total flux at 6700 Å (the mean wavelength of the photometric R band). Most of the secondary star features red-ward of Hα as well at the TiO 6159 Å band are removed, although some features in the blue wing of Hα remain. Thus, we conclude that the veiling factor, defined as the fractional contribution of the primary to the total light, is approximately 0.8 at λ = 6700 Å.

3.2. The orbital period

Using observations covering a time base of 814 days, Saffer et al. (1993) were able to measure the orbital period of PG0026+002 without aliasing problems as 0.5972570 $\pm$ 0.0000049 days. It is by far accurate enough to phase the current observations without cycle count ambiguities. This permits us to extend the time base for an improved period determination to 5116 days.

To do so, we measured the radial velocity (RV) of the narrow emission component of Hα. In order to remove possible distortions due to the underlying absorption, the absorption profile was first approximated by a spline fit, interpolating below the emission component. The division of the original spectrum by the spline yielded the rectified profile of the emission line. Its position was measured by a Gauss-fit. The derived RVs are listed in Table 2.

After applying the heliocentric correction, these RV data were combined with the data of Saffer et al. (1993; their Table 2) and with two further radial velocity measurements of Schultz et al. (1996). The entire data set was then investigated with the analysis-of-variance (AoV) method of Schwarzenberg-Czerny (1989). The resulting AoV periodogram permits to unambiguously determine the period P as 0.5972584 days. The distribution in time of the RV data of Saffer et al. (1993) and of Table 2 permits a natural grouping of the data into subsets, each one containing only data closely neighbouring in time. In a final step these subsets were fitted by sinusoids where the amplitude, systemic (γ) velocity and phase were left free to vary, but the period was fixed to the period of the peak of the AoV periodogram which is more than good enough for phase folding the subsets and keeping track of their cycle numbers. The resulting timings of the negative-to-positive γ crossing were then fitted by a linear relation, yielding the final value of the period P and the epoch T_0 of the γ crossing as quoted in Table 3. An $O-C$ diagram of the differences between the observed and the calculated epochs of γ crossing is shown in Fig. 4. The amplitude and the systemic velocity, also quoted in Table 3, were finally derived through a least squares sine fit to the entire data set, fixing P and T_0 to the previously found values. But note that K_2 and γ probably suffer from a systematic error as outlined in Sect. 3.3. The new orbital parameters are quite similar to those published by Saffer et al. (1993) but have a higher precision. The radial velocity curve, folded on the orbital period is shown in Fig. 5 together with a least squares sine fit.

The RVs measured by Wood et al. (1999) refer to Hβ instead of Hα. Therefore, they were not considered when the orbital parameters of PG1026+002 were revised. Nevertheless they agree very well with the Hα radial velocities and are therefore included in Fig. 5 as filled triangles[1].

Table 2. Radial velocities of the Hα emission component of PG1026+002

HJD Mid 2 450 000+	V_{obs} (km s^{-1})	orbital phase
863.647	−143.0	0.798
863.654	−158.6	0.809
863.662	−140.8	0.822
863.673	−148.1	0.840
863.684	−125.8	0.858
863.694	−120.3	0.876
863.709	− 98.5	0.901
863.719	− 85.2	0.919
863.730	− 71.1	0.937
863.746	− 51.5	0.963
863.757	− 25.5	0.981
863.768	− 14.6	0.999
863.779	10.5	0.017
864.660	− 2.0	0.493
864.671	− 28.0	0.511
864.684	− 34.5	0.533
864.695	− 33.1	0.551
864.705	− 72.0	0.569
864.718	− 94.0	0.590
864.729	−112.3	0.608
864.740	−120.5	0.626
864.752	−140.7	0.647
864.763	−143.4	0.665
864.773	−148.9	0.683
864.784	−161.3	0.701
864.794	−154.9	0.718
864.805	−157.7	0.735
865.711	165.0	0.253
865.722	171.8	0.271
865.733	165.4	0.289
865.767	142.9	0.346

Table 3. Revised orbital parameters of PG1026+002

Period P (days):	0.5972585	$\pm$ 0.0000002
Amplitude K_2 (km s^{-1}):	163.5	$\pm$ 1.2
Syst. velocity γ (km s^{-1}):	−8.9	$\pm$ 0.9
Phase T_0 (HJD):	2448511.1683	$\pm$ 0.0024

3.3. The emission line profile

In order to study the profile of the Hα emission component, the contribution of the secondary star was first removed from each

[1] It is not quite clear from the paper of Wood et al. (1999) if the RVs listed in their Table 4 contain the heliocentric correction. We presume that this is the case because otherwise they would deviate systematically from the Hα emission RVs.

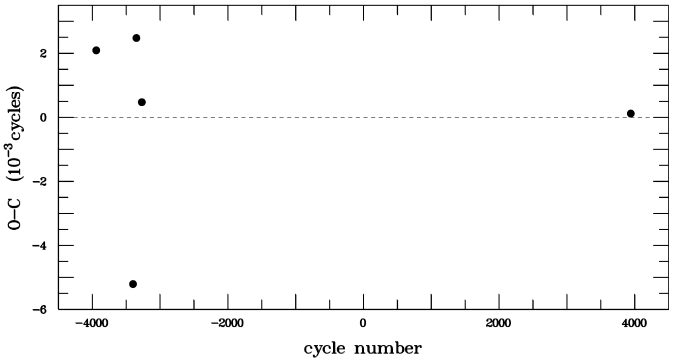

Fig. 4. $O-C$ diagram of the differences between the observed and calculated epoch of γ crossing of the Hα emission line radial velocities of PG1026+002.

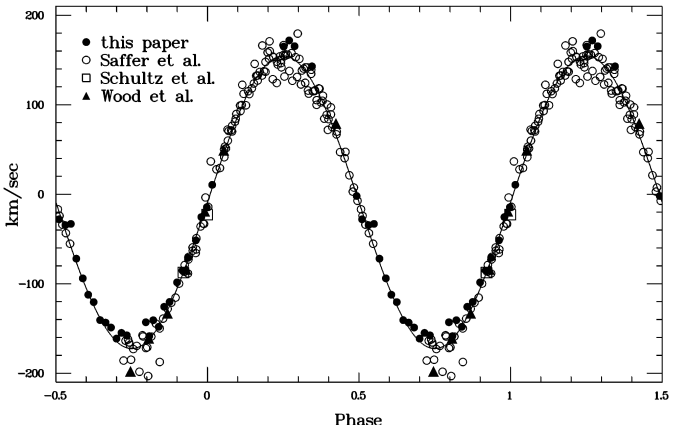

Fig. 5. Radial velocity curve of the narrow emission line component of Hα of PG1026+002, folded on the orbital period.

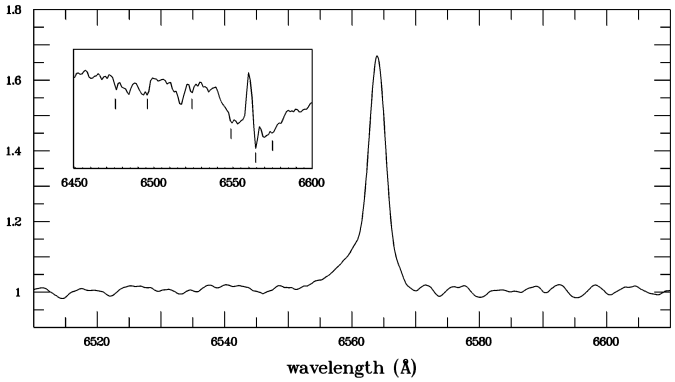

Fig. 6. Mean spectrum of the Hα emission component after removal of the secondary star spectrum and of the absorption component. The insert shows a sum of all spectra in the terrestrial rest frame with some water vapor absorption lines marked.

spectrum according to the veiling factor derived in Sect. 3.1. All spectra were then normalized to the continuum, regarding the Hα absorption profile as the local continuum. Subsequently, the spectra were shifted in wavelength in order to reduce them to the rest frame of the emission component.

After co-adding these spectra a narrow absorption component appeared in the red flanc of the line profile. This is probably a blend of telluric water vapor at 6564.2 Å and the sharp core of the Hα absorption of the white dwarf which is not easily removed by interpolating the spline fit to the total absorption profile beneath the emission component. The presence of water vapor lines can be seen in the insert in Fig. 6 which is a simple sum of all spectra in the terrestrial rest frame. Some telluric lines which are not severely blended with strong late type absorptions as seen e.g. in the spectrum of Yale 1755 are marked. However, although telluric features definitely contaminate the spectra, the absorption at 6564.2 Å is too strong to be soley explained by water vapor. Moreover, the minimum of the absorption corresponds to a RV of 20.7 km s^{-1}. This is in very good agreement with the expected mean velocity of 19.1 km s^{-1} of the white dwarf (taking into account the distribution of the observations in phase), assuming a mass ratio $M_2/M_1 = 0.34$ (Saffer et al. 1993), and supports the assumption that the absorption is dominated by the core of the Hα line of the white dwarf. In any case the sharp absorption is not part of the emission line profile.

In order to remove this feature, the normalized emission lines were co-added in the expected rest frame of the primary, calculated from the mass ratio of Saffer et al. (1993) and the values of K_2 and γ taken from Table 3. A spline was fitted to the mean emission profile, interpolating above the absorption component (tests with Gaussian profiles proved unsatisfactory). The difference between the spline and the original profile is considered as a fair approximation of the residual absorption component. If was shifted in wavelength according to the expected primary radial velocity and subtracted from the individual emission profiles. These were then again co-added in the rest frame of the secondary, yielding the mean profile shown in Fig. 6.

The shape of the emission consists basically of a narrow feature which in its main part is very well fitted by a Gaussian with $\sigma = 1.57$ Å. Comparing this to the instrumental line broadening as derived from the lines of the comparison spectra which can be considered to be intrinsically infinitely narrow this leads to a true linewidth of the emission component of 0.76 Å, corresponding to 35 km s^{-1}. This is in contrast to the results of Wood et al. (1999) who found the Hβ emission line in PG1026+002 to be intrinsically unresolved ($\sigma < 10$ km s^{-1}). However, it is in line with the intrinsic width of the emission components of the PCBs RE1016–053 and RE2013+400, also observed by Wood et al. (1999). We presume that the line width determined by Wood et al. (1999) is biased by the absorption core of the white dwarf for which they apparently did not correct their line profiles, and which could mimick a smaller emission line width. RE1016–053 and RE2013+400 are not subject to this effect because their Hβ emission lines are much stronger than that of PG1026+002. Thus, in contrast to the conclusion of Wood et al. (1999), the emission line width of PG1026+002 is not different from that in other PCBs.

Apart from the narrow Gaussian emission component there is a broad base on the blue flanc of the line. Regarding the individual spectra, it is not always visible. In order to investigate if

it appears preferably at certain orbital phases, the line profiles observed in the individual spectra were studied as a function of phase. The displacement of the line due to orbital motion is neatly visible on a corresponding plot, however, the limited signal-to-noise ratio makes it difficult to decide if there are significant phase-dependent variations in the emission profile.

The Hα absorption core of the white dwarf in the emission profiles raises concern as to which extent it can cause a systematic error of the measured RVs. In order to investigate this question radial velocities measured by Gauss fits to the emission profiles before and after subtracting the absorption core were compared. Least squares fits to the uncorrected and corrected RVs revealed an amplitude which is 10.6 km s^{-1} smaller after correction. The γ velocity is 3.7 km s^{-1} higher. Thus, any conclusions based on the dynamical properties of the secondary star as derived from the Balmer emission line component should take into account this correction.

3.4. The equivalent width of the Hα emission component

The emission components in the spectra of pre-cataclysmic binaries are generally interpreted as being due to re-processing of UV radiation of the hot primary in the atmosphere of the cool secondary (e.g. Thorstensen et al. 1978). They are thus restricted to the side of the secondary facing the primary. Depending on the orbital inclination of the system, its visibility from earth changes with orbital phase, leading to periodic variations of the equivalent width (EW) of the lines. Such an EW modulation was also observed by Saffer et al. (1993) in PG1026+002.

However, as Saffer et al. (1993) point out, the re-processing model does not work in the present case because the white dwarf in PG1026+002 is too cool and the component separation is too large for the secondary to intercept enough radiation of the primary to explain the observed EW variations of the Hα emission component. Saffer et al. (1993) favour intrinsic emission of the red dwarf. The modulation of its strength is then due to an asymmetric distribution of the emission on the stellar surface. The observed phasing being such that the emission comes predominantly from the side facing the primary can then be either due to some interaction with the white dwarf or it may be accidental. In the latter case Saffer et al. (1993) draw parallels to migrating waves seen in the light curves of many late type binaries. This hypothesis could be tested by measurements of the phasing of the EW curve at different epochs.

We therefore measured the EW of the Hα emission component in the present spectra. To minimize the influence of the secondary absorption spectrum, all spectra were first corrected for the veiling effect as measured in Sect. 3.3. The strength of the emission line was measured and referred to the strength of the local continuum interpolated above the broad absorption component to yield the EW (due to the non-photometric observing conditions, the observed line strength itself has no significance). These EW values were finally corrected for the contribution of the secondary which had been subtracted from the spectrum in order to refer it to the true continuum of the binary system. The resulting EW values, folded on the orbital period and binned in cells of $0.05\,P_{\rm orb}$ widths are shown in Fig. 7.

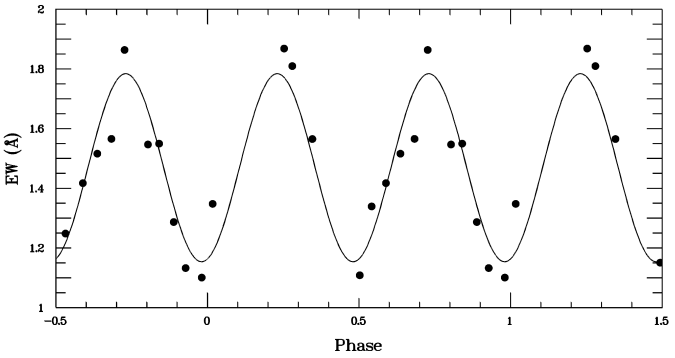

Fig. 7. The equivalent width of the Hα emission component of PG1026+002 (binned in cells of $0.05\,P_{\rm orb}$ width) as a function of orbital phase. The solid line is the best fitting sine curve with a period fixed at $0.5\,P_{\rm orb}$.

The EW definitely varies, however, not with the orbital period but it rather shows two minima and maxima per orbit. A least squares sine fit with the period fixed at $0.5\,P_{\rm orb}$ (solid line in Fig. 7), representing the observed data quite well, yields a mean EW of 1.45 $\pm$ 0.02 Å and an amplitude of 0.32 $\pm$ 0.02 Å (where the errors are formal fit errors). This is compatible with the observations of Saffer et al. (1993). The phase of the observations is such that the minima occur at orbital phases -0.02 and 0.48 (which in view of the uncertainties is definitely compatible with phases 0.0 and 0.5).

Thus, at the phases of upper and lower conjunction of the secondary star the EW assumes minima. This doublessly rules out re-processing of primary star radiation in the atmosphere of the red dwarf as the origin of the emission component (at least concerning the modulated part), confirming the view of Saffer et al. (1993). The maxima of the EW are seen when the line of sight forms a right angle with the line connecting the system components, i.e. when the secondary is seen sidewise. Thus, there seem to be two regions of enhanced emission roughly on opposite sides of the star.

But note that this view does not rule out a contribution to the Hα emission by reprocessing. In fact, as will be shown in Sect. 4, PG1026+002 exhibits a slight continuum variation which can very well be explained as being due to reflection. The favoured model requires a low orbital inclination. Thus, any modulation of a reflection induced emission line component would also be small (and diluted by the emission intrinsic to the red dwarf).

PG1026+002 is not the only pre-cataclysmic binary where the Hα emission component is not (exclusively) due to reprocessing of light of the primary white dwarf. Bruch (1999) recently showed that also in the system RR Cae – where the Hα emission has a considerably larger equivalent width than in the present case – the emission is intrinsic to the red dwarf. Thus, although there are doubtlessly pre-cataclysmic binaries where the emission is due to illumination, this is not a general rule in this kind of systems.

3.5. The Hα absorption line

Due to its broadness and the distortion of its shape by the light of the secondary, the radial velocity of the Hα absorption component is much more difficult to measure than that of the emission line. In order to remove the influence of the secondary absorption lines the spectrum of Yale 1755 was subtracted from the individual spectra of PG1026+002, considering the veiling factor derived in Sect. 3.1. In spite of normalizing the spectra to the continuum, masking the Hα emission component, smoothing the spectra by different degrees and applying several techniques for radial velocity measurements [Gaussian fits, cross-correlations, double Gaussian convolution (see Schneider & Young 1980)] in no case a convincing radial velocity curve resulted. There is a tendency for a variation in antiphase with the emission component at an amplitude which is not in contradiction with the expected amplitude, considering the mass ratio of 0.34 given by Saffer et al. (1993). However, the radial velocity curve is too noisy to permit more specific statements.

4. Photometry

4.1. The light curve

Time resolved photometry of PG1026+001 has not yet been published. The individual light curves obtained during the seven nights with photometric observations encompass between about 2.5 and 6 hours each. In most cases during this time a slight variation of the differential magnitude of PG1026+002 was visible. Since no such effect was observed for the magnitude differences between the various comparison stars, they can neither be attributed to variability of the latter nor to the non-photometric weather conditions prevailing during our observations, and must therefore be intrinsic to PG1026+002.

In order to reduce the scatter in the light curves, the data were binned into cells of 0.5 hours. An AoV periodogram (Schwarzenberg-Czerny 1989) of the combined light curves was calculated which revealed a period compatible with $P_{\rm orb}$. The light curve, folded on the orbital period, is shown in Fig. 8. Data of different nights are plotted with different symbols. Obviously, PG1026+002 exhibits sinusoidal variations with a very small amplitude, of the order of $0\overset{\rm m}{.}01$. A sine curve with the period fixed at $P_{\rm orb}$ was fitted to the data, yielding a half-amplitude of $0\overset{\rm m}{.}0063 \pm 0\overset{\rm m}{.}0005$. The minimum occurs at orbital phase 0.07 ± 0.01. The formal error definitely underestimates the true uncertainty. Systematic effects such as a different zero point of the magnitude differences in different nights due e.g. to different colours of PG1026+002 and the primary comparison star in combination with variations of the mean extinction can explain the observed phase shift: Assuming for example a shift in $\Delta{\rm m}$ of $-0\overset{\rm m}{.}005$ for the data of February 2 (and disregarding the two outliers of February 3) a least squares fit yield a phase of minimum within 1σ of phase 0. Alternatively (or additionally) a slight intrinsic variability of the secondary due to the active regions on its surface, which are doubtlessly present as indicated by the equivalent width variations of the Hα emission,

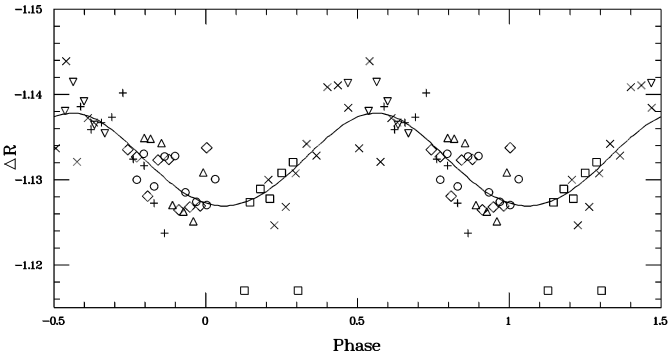

Fig. 8. Light curve of PG1026+002 (dots) folded on the orbital period. Data of different night are represented by different symbols: 1998, Feb. 1 (+), Feb. 2 (×), Feb. 3 (□), Feb. 4 (△), Feb. 5 (▽), Feb. 7 (◇), Feb. 19 (◯). The solid line is a synthetic light curve calculated with the Wilson-Devinney code.

might cause a distortion of the light curve. Therefore, before the reality of the phase shift of the light curve minimum away from phase 0 is confirmed by independent observations, for the sake of interpreting the magnitude variations we will assume that this shift is not significant.

If this assumption is true, the variations can qualitatively be understood as a classical reflection effect: Phase 0 is the epoch of lower conjunction of the secondary. Half a period later the illuminated side of the red dwarf is best visible, giving rise to the observed maximum in the light curve. In order to verify if a viable model of PG1026+002 based on this idea can be constructed, we will now proceed to perform a quantitative analysis of the light curve, using the Wilson-Devinney (WD) light curve synthesis routine (Wilson & Devinney 1971, Wilson 1979) as implemented in the MIRA image processing system.

4.2. Light curve synthesis

In view of the exceedingly small amplitude of the variations and the corresponding scatter of the data points it is not sensible to use the WD routine in order to fit a model light curve to the data by varying the numerous parameters which determine its shape: parameter correlations would permit a large volume within the multidimensional parameter space to lead to equally acceptable solutions. However, if the parameters can be constrained by independent reasoning it can be tested if the predicted light curve is in agreement with the observations.

Within a reflection model the shape of the light curve is essentially determined by the following parameters. (a) The orbital inclination i: Saffer et al. (1993) found $\sin i = 0.93 \pm 0.56$ which translates into $i > 22°$. The absence of eclipses implies $i \lesssim 85°$. Thus, i is only poorly constrained. (b) The primary temperature T_1: following Kepler & Nelan (1993) we adopt $T_2 = 19\,900 \pm 390$ K. (c) The secondary temperature T_2: Leggett et al. (1996) adjusted stellar atmophere models to cool dwarfs. From their results the relation $T[{\rm K}] = (3907 \pm 24) - (184 \pm 6)\,S$ can be derved, where S is the spectral subtype for M stars. For $S = 4 \pm 0.25$ (Saffer et al.

1993), $T_2 = 3170 \pm 50$ K. (d) The component separation a: It is easily calculated from the RV amplitude of the secondary, the orbital period and the mass ratio (see below), if a specific value for the orbital inclination is adopted. (e) The primay radius R_1: Saffer et al. (1993) used their value of $\log g$ and evolutionary models of Wood (1990) to derive the primary mass. For consistency we use this mass together with g to calculate $R_1 = 0.0119^{+0.0030}_{-0.0019}\,R_\odot$. This value is identical to what is calculated from the mass-radius relation of Nauenberg (1972), allowing for a small non-degenerate hydrogen layer on the white dwarf (Koester & Schönberner 1986). (f) The secondary radius R_2: Regarding both components as black bodies we calculate the surface flux at the mean wavelength of the R band. The condition that the fluxes of both components, multiplied by their surface areas, should lead to the observed veiling factor leads to $R_2 = 0.40\,R_\odot$. This radius is larger than that derived using M_2 and empirical mass-radius relationships (0.25 $R_\odot$: Lacy 1977; 0.28 $R_\odot$: Caillaut & Patterson 1990) or theoretical model calculations (0.26 $R_\odot$: Neece 1984; 0.24 $R_\odot$: Burrows et al. 1993, slightly extrapolating their tables). However, as a consequence of a previous common envelope evolution the PG1026+002 secondary may not conform to the usual mass-radius relationship for lower main sequence stars: An excessively large radius has recently been found by Bruch (1999) for the secondary star of another pre-cataclysmic binary, RR Cae. Here, we adopt the larger radius of 0.40 $R_\odot$, noting that this choice is not critical for the results. (g) The mass ratio q: Adopting the component massed derived by Saffer et al. (1993), the mass ratio is $q = 0.34 \pm 0.14$. (h) The atmospheric parameters albedo A, gravity darkening exponent β and limb darkening coefficient μ: For the primary these have no bearing on the modelling of the light curve because of the compactness of the white dwarf. For the secondary we take $A_2 = 0.56$ (Rafert & Twigg 1980), $\beta_2 = 0.32$ (Lucy 1967) and an arbitrary but not unreasonable value of $\mu_2 = 0.9$, the light curve not depending strongly on μ_2.

Using the parameters listed above, permitting only the orbital inclination (and the normalization magnitude) to be adjusted, the WD routine was employed to calculated a synthetic light curve for the system. A phase shift was introduced in order to allow for the apparent offset of the minimum in the light curve from the expected phase 0 (see Sect. 4.1). Choosing $i = 35°$ resulted in the light curve shown as a solid line in Fig. 8. It fits the data as good as can be in view of the observational scatter. The R-statistics (Bruch 1999) yield only a 7% probability for any residual non-random variations of the $O-C$ curve between data and model. In view of the fact that apart from the trivial normalization constant the model contains only one free parameter (the orbital inclination) this is a remarkably good agreement with the data.

Thus, a simple reflection model is capable to quite satisfactorily explain the brightness modulations of PG1026+002. Moreover, the adopted parameters are reasonable. However, the success of the above exercise does not mean that our choice of parameters is unique. Changing one or the other parameter within the wide error ranges quoted above, and repeating the model calculations, shows that with appropriate modifications of other parameters a good fit to the observed data can in general also be achieved. Therefore the light curve synthesis can only confirm the plausibility of the dynamical and physical model of PG1026+002 as defined by the adopted parameter set but cannot improve their numerical values.

5. Conclusions

We have presented time resolved spectroscopic observations of the pre-cataclysmic binary PG1026+002. The analysis of the spectra confirms the model elaborated by Saffer et al. (1993). In particular, the phase dependence of the variations of the equivalent width of the Hα emission components definitely proves that the emission (at least the modulated part) is not due to illumination of the secondary star by the white dwarf, but is intrinsic to the M dwarf itself. At the epoch of the present observations two activity centres appear to be present on opposite sides of the star and perpendicular to the line connecting the system components. Our observations increase the total time base over which radial velocity measurements are available by a factor of 6. In consequence a correspondingly more accurate value for the orbital period could be derived. Revised ephemeris are given.

In addition to the spectroscopy the first time resolved photometric observations of PG1026+002 are presented. Very slight quasi-sinusoidal variations at the orbital period are observed. The half-amplitude is only of the order of $0\overset{\mathrm{m}}{.}006$. We interpret them as due to light of the primary reflected off the red dwarf. Although the scatter in the light curve is too large to permit a determination of the system parameters via an adjustment of a model light curve to the data, a light curve calculated with the Wilson-Devinney code based on system parameters taken from Saffer et al. (1993) and on additional information from our spectroscopic observations fits the observed light curve excellently, showing that the adopted system parameters are reasonable.

Acknowledgements. We are grateful to Dr. L.P.R. Vaz for making his version of the Wilson-Devinney code available to us. This work was partially supported by grants of the Conselho Nacional de Pesquisa (CNPq; grants Nos. 301029 and 301784), and the Fundação Amparo a Pesquisa de Minas Gerais (FAPEMIG; grant No. 205096).

References

Bruch A., 1993, *MIRA – A reference guide* Universität Münster
Bruch A., 1999, AJ 117, 3031
Burrows A., Hubbard W.B., Saumon D., Lunine J.E., 1993, ApJ 406, 158
Caillaut J.-P., Patterson J., 1990, AJ 100, 825
Fabrika S.N., Shtol' V.G., Valyavin G.G., Bychkov V.D., 1997, Pis'ma Astron. Zh. 23, 47
Fleming T.A., Liebert J., Green R.F., 1986, ApJ 308, 176
Green R.F., Schmidt M., Liebert J., 1986, ApJS 61, 305
Hamuy M., Walker A.R., Suntzeff N.B., et al., 1992, PASP 104, 533
Jacoby G.H., Hunter D.A., Christan C.A., 1984, ApJS 56, 257
Kepler S.O., Nelan E.P., 1993, AJ 105, 608
Koester D., Schönberner D., 1986, A&A 154, 125

Lacy C.H. 1977, ApJS 34, 479
Landau L.D., Lifshitz E.M., 1951, The Classical Theory of Fields (Oxford: Pergamon)
Leggett S.K., Allard, F., Berriman G., Dahn, C.C., Hauschildt P.H., 1996, ApJS 104, 117
Lucy L.B., 1967, Z. Astrophys. 65, 89
Nauenberg M., 1972, ApJ 175, 417
Neece G.D., 1984, ApJ 277, 738
Rafert J.B., Twigg L.W., 1980, MNRAS 193, 76
Saffer R.A., Wade R.A., Liebert J., et al., 1993, AJ 105, 1945
Schneider D.P., Young P., 1980, ApJ 238, 946
Schultz G., Zuckerman B., Becklin E.E., 1996, ApJ 460, 402
Schwarzenberg-Czerny A., 1989, MNRAS 241, 153
Sion E.M., Fritz L.M., McMullin J.C., Lallo M.D., 1988, AJ 96, 251
Thejll P., Flynn C., Williamson R., Saffer R., 1997, A&A 317, 689
Thorstensen J.A., Charles P.A., Margon B., Bowyer S., 1978, ApJ 223, 260
Wilson R.E., 1979, ApJ 234, 1054
Wilson R.E., Devinney E.J., 1971, ApJ 166, 605
Wood J.H., Harmer S., Lockley J.J., 1999, MNRAS 304, 335
Wood M., 1990, Ph.D. thesis, University of Texas